



Supplement of

How does cloud-radiative heating over the North Atlantic change with grid spacing, convective parameterization, and microphysics scheme in ICON version 2.1.00?

Sylvia Sullivan et al.

Correspondence to: Sylvia Sullivan (sylvia@arizona.edu) and Aiko Voigt (aiko.voigt@univie.ac.at)

The copyright of individual parts of the supplement might differ from the article licence.

Table S1. Cloud fraction values in the HIGH, MIDDLE, and LOW altitudinal ranges using three sets of percentiles across simulations of different grid spacings with the one-moment microphysics.

	80 km	40 km	20 km	10 km	5 km	2.5 km	2.5 km - shcon
Set 1 - HIGH: 62nd perc, MID: 67th perc, LOW: 30th perc							
HIGH	12.1	25.8	30.5	37.4	40.3	47.0	39.3
MID	11.0	24.9	30.5	45.0	42.5	56.6	51.3
LOW	10.0	8.0	7.0	8.0	6.2	5.6	4.5
Set 2 - HIGH: 60th perc, MID: 60th perc, LOW: 25th perc							
HIGH	4.1	13.0	17.9	31.6	29.3	33.9	26.9
MID	3.1	6.4	7.3	8.7	8.2	17.8	8.3
LOW	6.0	3.4	2.2	2.5	1.6	1.1	0.8
Set 3 - HIGH: 65th perc, MID: 70th perc, LOW: 35th perc							
HIGH	30.2	41.7	47.1	52.5	54.6	58.2	54.7
MID	19.8	50.0	51.0	54.9	54.4	66.9	59.3
LOW	14.0	12.5	11.9	13.6	11.7	12.1	5.2

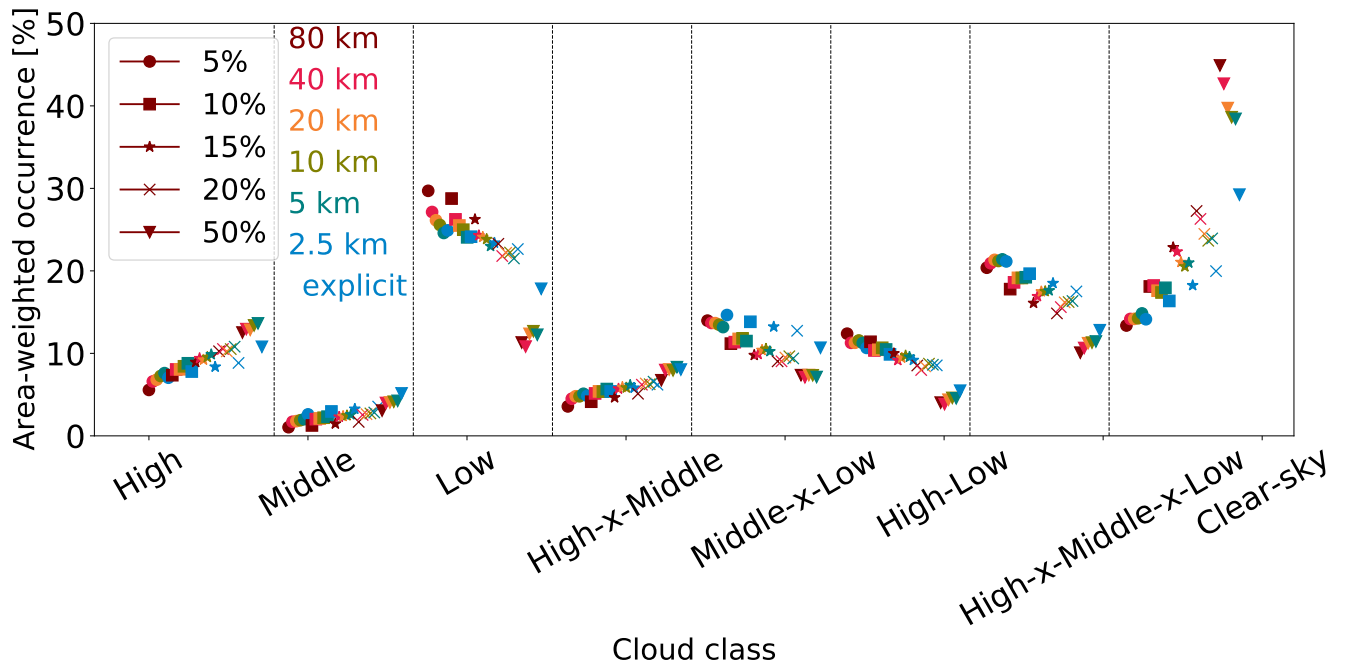


Figure S1. Occurrence probability is relatively insensitive to the cloud fraction threshold used to define various classes. Mean, area-weighted occurrence probabilities for eight cloud classes across grid spacings for the simulations with two-moment microphysics. Different symbols indicate different cloud fraction thresholds for Low, Middle, and High altitudinal ranges to qualify as cloudy. Different colors are grid spacings from 80 km down to 2.5 km, as in Fig. 7.

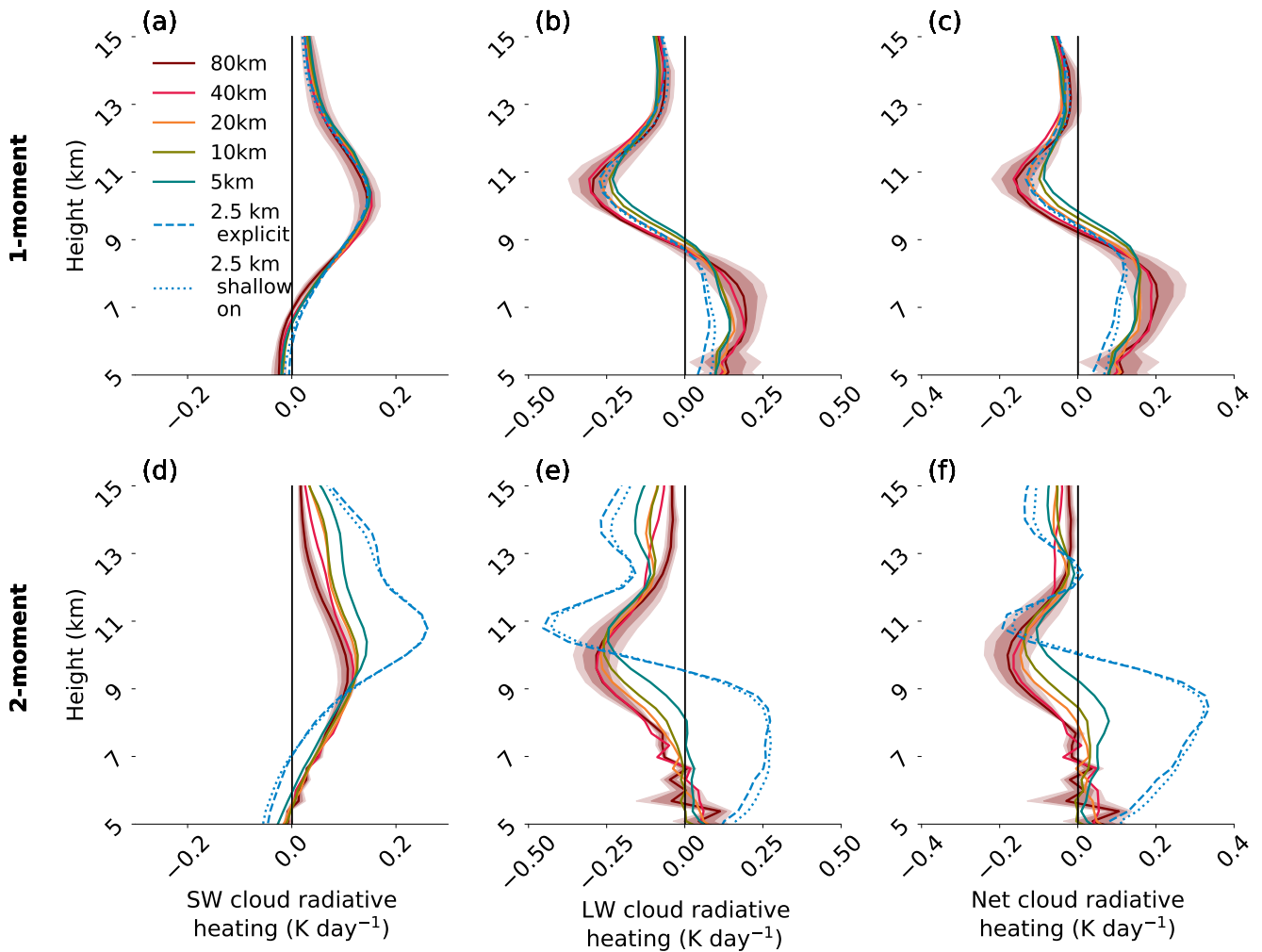


Figure S2. Dependency of net, shortwave, and longwave cloud-radiative heating on grid spacing, convective scheme, and microphysics is robust to simulation duration. Upper-tropospheric, time mean, area mean shortwave (left panels), longwave (middle panels), and net (right panels) cloud-radiative heating with all model settings as in Fig. 5. One- (top panels) and two-moment (bottom panels) microphysics scheme are shown. Note the different x-axis limits on each set of panels. The standard deviation and standard error over daily means are depicted as light and dark red shades atop the 80-km profile.

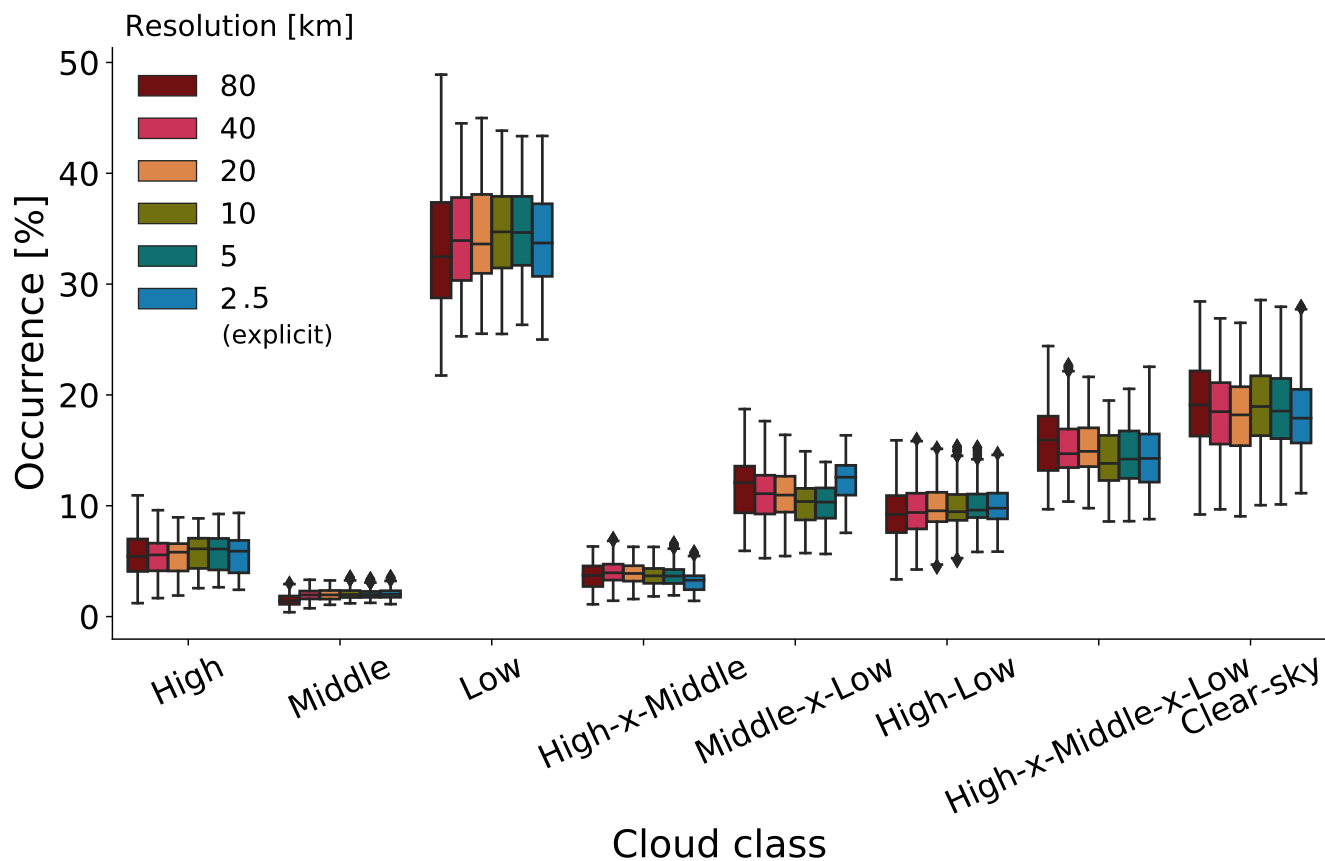


Figure S3. There are no systematic changes in cloud class occurrence with grid spacing. Area-weighted occurrence probability for eight cloud classes across grid spacings for the simulations with one-moment microphysics. The box shows 25th (Q1), 50th (Q2), and 75th (Q3) percentiles, while the whiskers show $Q1-1.5(Q3-Q1)$ up to $Q3+1.5(Q3-Q1)$. Diamonds indicate outliers. Thresholds of 62%, 67%, and 30% are used for high, middle, and low clouds, but mean occurrence is not sensitive to these thresholds (Fig. S1). The 2.5-km simulation uses neither a deep nor shallow convective parameterization (explicit).

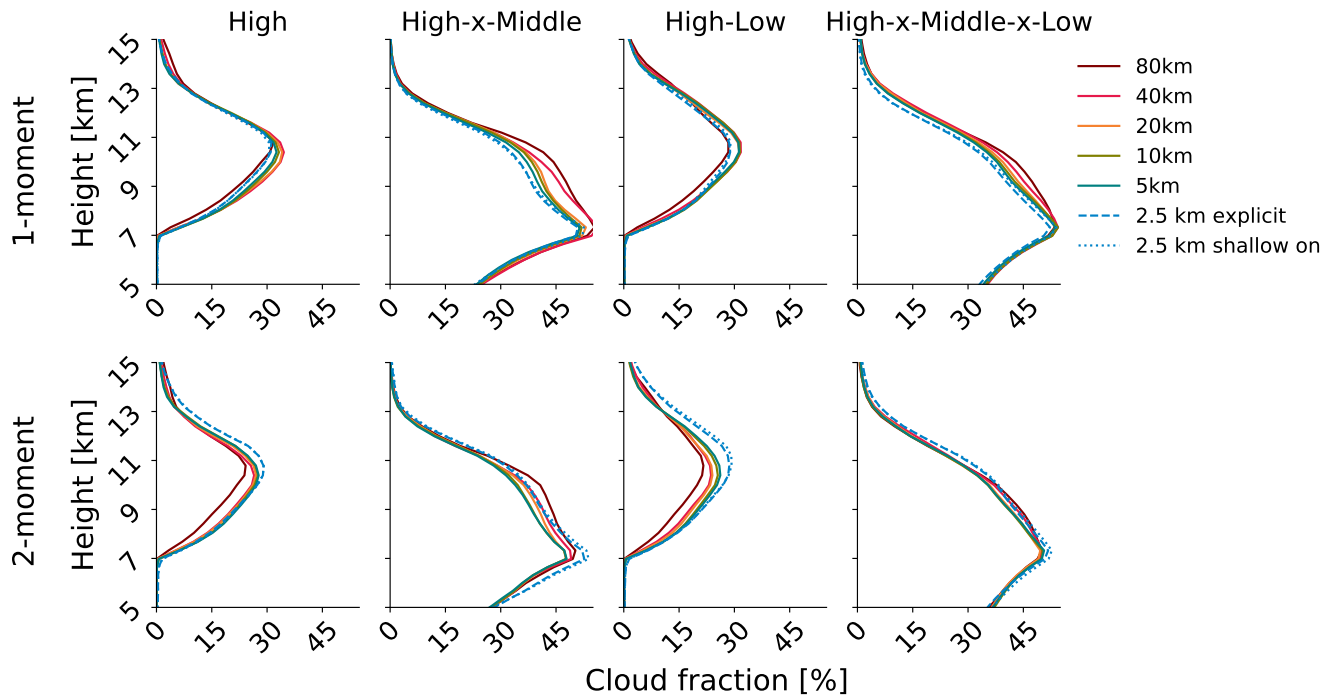


Figure S4. Cloud fraction does not change much with grid spacing across all classes with high clouds. Cloud fraction from one- (top panels) and two-moment (bottom panels) simulations for the four cloud classes that include high clouds with all model settings as in Fig. 5.

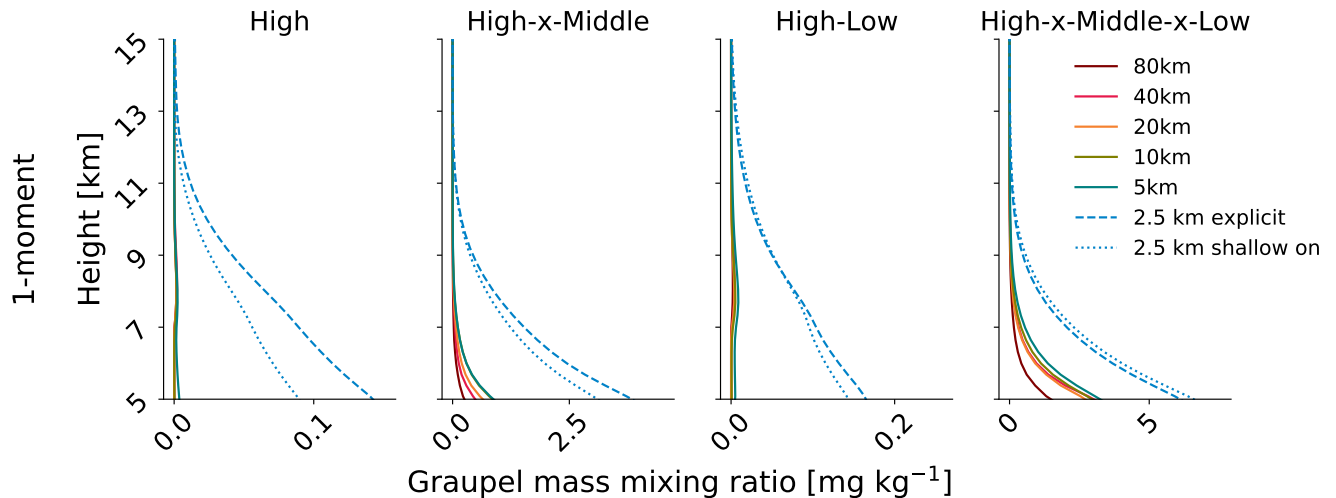


Figure S5. Grid spacing dependence for the one-moment microphysics simulations is concentrated in a radiatively inactive species. Graupel mass mixing ratios from the one-moment simulations for the four cloud classes that include high clouds with all model settings as in Fig. 5.